Available online at www.sciencedirect.com

ScienceDirect

Procedia Engineering 183 (2017) 219 – 226

Procedia Engineering

www.elsevier.com/locate/procedia

17th International Conference on Sheet Metal, SHEMET17

Disk-laser welding of Ti-6Al-4V titanium alloy plates in T-joint configuration

F. Caiazzo[a,*], F. Cardaropoli[a], V. Alfieri[a], V. Sergi[a], P. Argenio[a], G. Barbieri[b]

[a]*Department of Industrial Engineering, University of Salerno, Via Giovanni Paolo II 132, 84084 Fisciano (SA), Italy*
[b]*Consorzio Calef C/O CR ENEA Trisaia, SS106 Ionica Km 419.500, 75026 Rotondella (MT), Italy*

Abstract

Titanium alloys are employed in a wide range of applications, ranging from aerospace to medicine. In particular, Ti-6Al-4V is the most common, thanks to an excellent combination of low density, high specific strength and corrosion resistance. Laser welding has been increasingly considered as an alternative to traditional techniques to join titanium alloys. An increase in penetration depth and a reduction of possible welding defects is indeed achieved; moreover a smaller grain size in the fused zone is benefited in comparison to either TIG and plasma arc welding, thus providing an increase in the tensile strength of the welded structures.

The aim of this work is to study disk-laser welding of 3.2 mm thick Ti-6Al-4V plates in T-joint configuration without using a filler wire, defining the influence of different process parameters. The issue concerning the clamping of the plates is discussed and a proper device is developed to carry out welds.

A structured plan has to be carried out in order to characterize the process thus discussing the response variables. Power and welding speed are considered as crucial input variables since they determine the thermal input to the work-piece; furthermore, given the particular configuration analyzed, tilt angle is considered as a further variable, whereas focus position is fixed below the upper surface to obtain a full penetration.

Welding beads have been first examined with a coordinate measuring machine to study distortions, and then from a morphological point of view. Eventually, Vickers microhardness testing has been conducted to discuss structural changes in fusion and heat affected zone due to welding thermal cycles.

Peer-review under responsibility of the organizing committee of SHEMET17

Keywords: disk-laser welding; Ti-6Al-4V; T-joint configuration.

* Corresponding author. Tel.: +39-089-964323.
E-mail address: f.caiazzo@unisa.it

Peer-review under responsibility of the organizing committee of SHEMET17
doi:10.1016/j.proeng.2017.04.024

1. Introduction

Titanium alloys are widely employed in the aerospace sector, due to high strength in combination with low density and good tensile properties; moreover, resistance to corrosion allows applications in chemical aggressive conditions [1]. In particular, Ti-6Al-4V accounts for more than half of all titanium tonnage in the world and no other titanium alloy is deemed to threaten its dominant position [2]. The use of Ti-6Al-4V alloy is diffused in aerospace for turbine disks, compressor blades, airframe and space capsule structural components, rings for jet engines, pressure vessels, rocket engine cases, helicopter rotor hubs, fasteners, and engine exhausts. Medical and surgical devices are also produced with this alloy [3]. Ti-6Al-4V is a two phase α-β alloy, with aluminum as the alpha stabilizer and vanadium as the beta stabilizer. The nominal chemical composition [1] is listed in Table 1. Strengthening is achieved through heat treatment or thermomechanical processing, although the best combination of properties results from solution heat treatment and consequent rapid quenching and aging [2]. As a consequence of welding thermal cycles, a significant variation of microstructure is noticed in the welding bead. A specific mechanic performance of the bead is expected depending on the microstructure [4].

Laser welding is considered as an alternative to the traditional techniques to join plates of titanium alloys for industrial applications and systems [5]. The particular advantages of this process are in an increased depth of penetration and a reduction of possible welding defects and of melted and heat affected zone compared to a TIG or plasma arc welding, thus entailing an increase in mechanical performances of welded structures [6,7]. Another innovative method of welding with highly concentrated energy source is electron beam [8], but this technique presents the disadvantage that vacuum is needed; in addition, the process involves X-rays emission.

Table 1. Nominal chemical composition of Ti-6Al-4V alloy (wt.%).

Al	V	Fe	O_2	H_2	C	N_2	Ti
5.5 ÷ 6.8	3.5 ÷ 4.5	<0.4	<0.2	<0.015	<0.08	<0.05	Balanced

Few studies are available in literature on laser welding of titanium alloy T-joints. To obtain T-joints several laser welding configurations can be adopted: double-sided, single-sided, simultaneous or successive passes. Wang manufactured welds without defects using the full penetration laser-TIG hybrid welding technique through the skin plate [9]. This method could be not adequate if a higher quality is necessary on the skin, and involves post process operations to remove imperfections. Spina analysed bead microstructure and mechanical properties of double-sided hybrid laser arc welding Ti–6Al–4V T-joints in two passes [10]. Kashaev studied Nd:YAG single-sided laser beam welding of Ti–6Al–4V 2.5 mm thick T-joints with a compatible filler (Titanium Grade 2). The use of filler is justified by avoiding underfills and undercuts. Moreover, the author defined suitable process parameters to obtain full penetration, but observed that the performance of T-joint is sensible to weld shape and morphology, and fracture always occurred in the weld [11]. Ma made T-joints of Ti–6Al–4V alloy with double-sided synchronized laser beam welding with homologous filler wire. The author reported that weld seams are characterized by good quality without surface defects or discontinuity. Besides that, tensile tests showed that fracture occurred in the base material, due to strengthening effect of the martensite in heat affected and fused zone [12].

This paper aims to study disk-laser welding of 3.2 mm thick Ti-6Al-4V plates in T-joint configuration without using a filler wire, defining the influence of different process parameters. In particular, a Yb:YAG diode-pumped thin disk-laser source is employed: advantages arise indeed, as a consequence of only weak thermal lensing effects; better beam quality is benefited because the divergence and the diameter variation along the propagation axis decrease [13]. Furthermore, a proper device is intended to be developed to clamp the plates in an adequate way.

2. Design of Experiments

Basing on the literature and past experience, a proper choice of the governing parameters is carried out [14,15]. Laser power and welding speed are crucial factors as they determine heat input on the work-piece [16], so they have to be taken into account in the study. Nevertheless, power and speed levels are subject to the defocusing [17]. In fact, in order that the beam would interest a larger area, it was employed a defocused beam. This choice guarantees the production of a bead with a wider crown and ensure greater resistance in T-joint configuration; in particular, a 3

mm negative defocusing has been adopted, because it has been associated with a reduction of the grain size in a previous work [18]; the growth in grain size would otherwise produce a decrease in the tensile strength of the welded structures [19]. As a result of defocusing irradiance decreases; in order to overcome the specific threshold irradiance for key-hole welding, it is therefore necessary to adopt higher values of power and minimum speed values. Moreover, given the particular configuration examined, it has been decided to investigate the effect of the tilt angle. The choice of levels for the beam angle is dictated by the practical positioning of head and assistance gas apparatus for the prevention of oxidation; this narrows the possible angle range. It has then been chosen to use 30° and 45° tilt angles.

A full two-level experimental plan with power (P), speed (s), and beam angle (α) as governing factors has been arranged (Figure 1) with three replications to check the statistical significance of the responses; testing conditions are summarized in Table 2. A random test procedure has been arranged both to allocate the plates and produce the specimens, so that the observations are independent random variables, aiming to reduce systematic experimental variation.

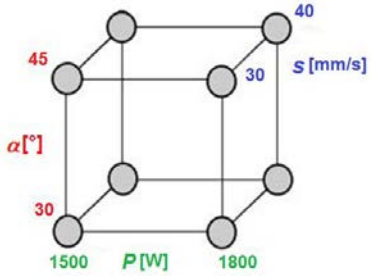

Fig. 1. Scheme of the experimental plan.

Table 2. Testing conditions in the experimental plan.

Condition	Tilt angle [°]	Power [W]	Welding speed [mm/s]	Heat input [J/mm]
A	30	1500	30	50.0
B	30	1500	40	37.5
C	30	1800	30	60.0
D	30	1800	40	45.0
E	45	1500	30	50.0
F	45	1500	40	37.5
G	45	1800	30	60.0
H	45	1800	40	45.0

Welding beads have been first examined with a coordinate measuring machine to study distortions, and then from a morphological point of view. Two groups of geometric responses (Figure 2) have been investigated, the former including responses concerning the bead shape; the latter considering possible imperfections as suggested by AWS specification [20].

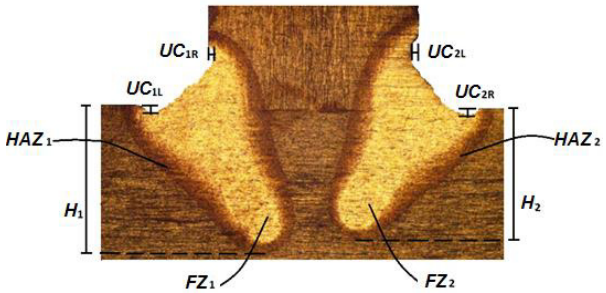

Fig. 2. Responses concerning bead shape and imperfections.

Concerning geometrical dimensions, the responses are the penetration depth (H), the area of heat affected zone (HAZ) and the area of fused zone (FZ). Relating to the bead imperfections, the evaluation included right and left undercuts (UC).

3. Experimental Procedure

The study has been carried out on 3.2 mm thick Ti-6Al-4V plates in T-joint configuration. The schematic illustration and relative dimensions of the joint are shown in Figure 3. Welding has been performed in continuous wave emission using a Trumpf TruDisk 4002, Yb:YAG diode-pumped thin disk laser source. 100 mm long welding beads have been produced in two passes, one for each side of the stringer. A Trumpf BEO D70 focusing optics

welding head, moved by an ABB IRB 240 M2004 robot, has been used to produce the samples. To solve the issue concerning the clamping of the plates, a specific jig has been developed. It consists of two parts at adjustable distance with seats for sheet positioning, in order to obtain the correct assembly; the system is completed by clamping clips (Figure 4).

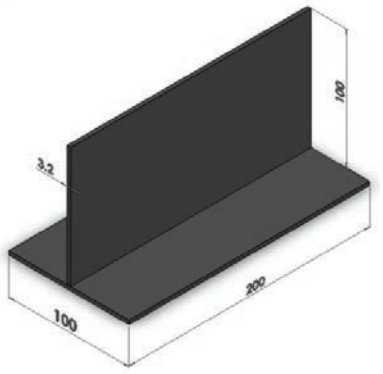

Fig. 3. Schematic illustration and relative dimensions (in mm) of the joint.

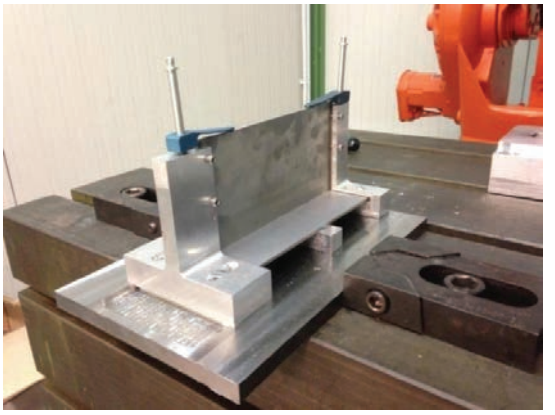

Fig. 4. Jig for T-joint welding.

As bead shielding is crucial in order to obtain sound joints when processing titanium alloys, surface protection is ensured by the use of a device integrated in the welding head, with the distribution of argon flow with a rate of 25 l/min; the removal of the plasma during vaporization is obtained with a leading nozzle supplying helium with a flow rate of 30 l/min. Given the particular configuration of the joint, it is not necessary back-side shielding.

In the field of laser welding and considering aerospace applications, the preparation of the joints to ensure proper matching of the surfaces and remove foreign particles which could contaminate the melt pool is relevant. Therefore, any burrs have been removed with abrasive paper and the surfaces have been pickled with a solution of nitric and hydrofluoric acid.

After welding, joints have been subjected to visual inspections and beads have been examined with a coordinate measuring machine to study distortions. Then samples have been cross cut perpendicularly to the welding direction and then polished to a mirror finish with SiC paper and grinding diamond paste on polishing cloths. Chemical etching has been performed using hydrofluoric acid (48%, 10 ml), nitric acid (65%, 15 ml), and water (75 ml) at room temperature in order to highlight the bead boundaries and the microstructure in the cross section [1].

4. Results and Discussion

Visual inspections have been conducted in order to check the effectiveness of the device for bead shielding. Discoloration of the bead would suggest that oxidation took place during the process; in particular, an inadequate flow rate would have resulted in the formation of blue or yellow spots. Beads are found to be uniform, smooth, and silvery, and no spatters are observed. Therefore, bead protection has been considered adequate.

As an example, in Figures 5 (a-b) bead aspect of the two tracks obtained in condition B are shown. Figures 6 (a-b) display the corresponding magnifications acquired through a stereoscopic microscope.

The characteristic angles of distortion (Figure 7) produced by the thermal deformation of each sample have been evaluated by a coordinate measuring machine. The average values obtained for replications of each condition are reported in Table 3.

From the values determined for the angle δ, it is apparent that the plate presents a deformation which compromises the flatness. In particular, assuming a nominal starting angle of 180°, a maximum reduction of 3° is noted. Furthermore, from the analysis of γ_1 and γ_2 it is observed that the production of the two tracks determines an asymmetry of the joint because during the execution of the second track the material undergoes a further deformation due to the release of residual stress accumulated in the execution of the first track, in addition to the thermal deformation due to the passage of the laser source; for this reason, regardless of the test condition, $\gamma_1 > \gamma_2$.

Thermal distortion is a function of thermal input: the angle δ decreases with increasing heat input, as shown in the graph in Figure 8.

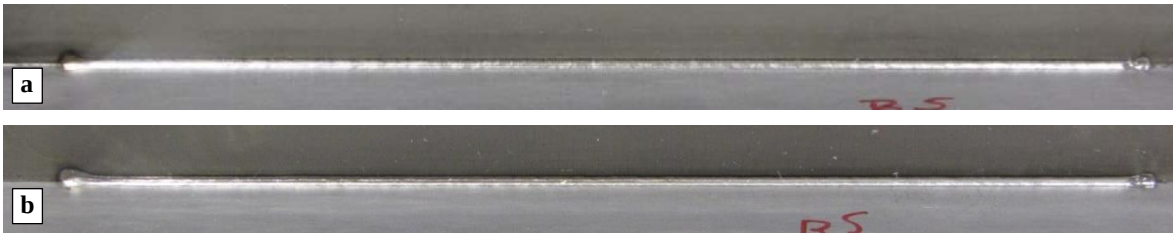

Fig. 5. Bead aspect obtained in condition B: first track (a), second track (b).

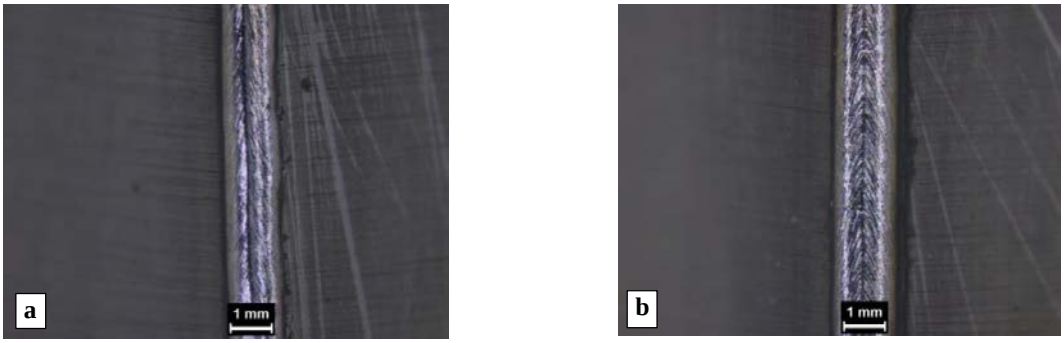

Fig. 6. Magnification of bead aspect obtained in condition B: first track (a), second track (b).

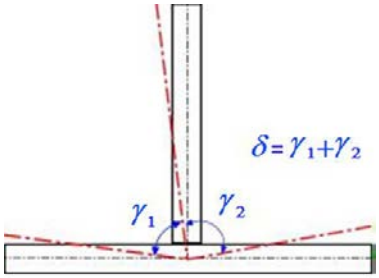

Fig. 7. Definition of distortion angles.

Table 3. Distortion angles of T-joint samples.

Condition	γ_1	γ_2	δ
A	89.035	88.630	177.665
B	89.374	88.845	178.219
C	88.705	88.755	177.460
D	88.961	88.947	177.908
E	89.325	88.506	177.831
F	89.273	88.929	178.202
G	89.432	88.400	177.832
H	88.957	88.964	177.921

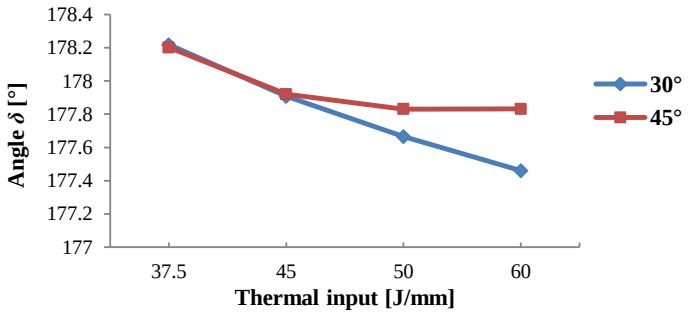

Fig. 8. Angle δ as a function of thermal input.

The samples have been sectioned perpendicularly to the welding direction. Examples of bead cross sections in welding conditions B and G are shown in Figures 9 and 10. These macrographs have been chosen because represent the different behaviors observed changing welding parameters.

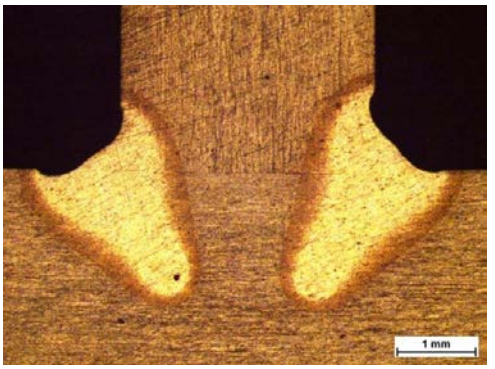

Fig. 9. Macrograph of bead cross section in condition B.

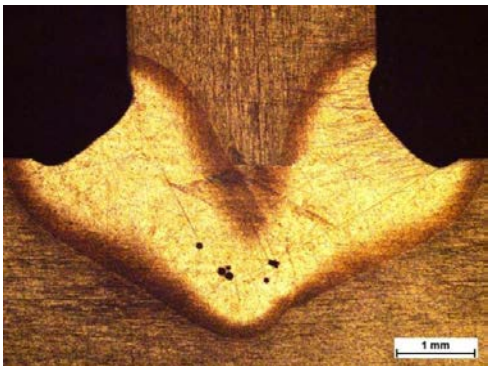

Fig. 10. Macrograph of bead cross section in condition G.

The bead cross sections are characterized by some pores, due to trapped gas within the solidifying welding pool, but their size fulfills the requirements of AWS D17.1: 2010 [20]. By optical microscopy it is possible to highlight the presence of three areas: base metal, heat affected and molten zone. The base metal is composed of a β phase (which appears dark in the macrographs) in a matrix α (bright), which is the typical structure of the alloy that has undergone an annealing process, not altered by welding. The heat affected zone is a mixture of α' and α phases. This corresponds to a structure which is quenched below the β-transus ranging from 720 to 985 °C [2]. The molten zone, instead, mainly consists of acicular martensite α'. A similar structure is obtained when quenching the alloy from the β phase region above the β-transus, which is 985 °C approximately. It has to be assumed that a value of 410 °C/s, required to attain a completely martensitic microstructure for Ti-6Al-4V alloy, is overcome.

Based on the general aspect of the welding bead, two groups of geometric responses have been investigated concerning bead shape and imperfections. Average responses among three cross sections for each tested condition are given in Table 4. It is worthwhile to notice that the melted zones obtained in conditions G and H, namely with the maximum power and tilt angle of 45°, are crossing; therefore, only a measure is reported for fused and heat affected zones.

Table 4. Average values of geometric features and imperfections of welding beads.

Condition	H_1 [mm]	H_2 [mm]	FZ_1 [mm^2]	FZ_2 [mm^2]	HAZ_1 [mm^2]	HAZ_2 [mm^2]	UC_{1L} [mm]	UC_{1R} [mm]	UC_{2R} [mm]	UC_{2L} [mm]
A	2.12	2.15	2.78	2.9	4.7	5.15	0.16	0.05	0.06	0.08
B	1.81	1.85	2.13	2.33	3.63	3.74	0.12	0.05	0.04	0.09
C	2.45	2.49	4.15	3.94	6.57	5.82	0.09	0.07	0.12	0.06
D	2.3	2.02	2.72	2.74	4.79	4.43	0.07	0.04	0.04	0.1
E	1.88	1.52	3.45	3.49	4.85	4.99	0.14	0.05	0.06	0.07
F	1.6	1.15	2.32	2.28	3.91	3.27	0.05	0.06	0.08	0.05
G	2.23	2.23	7.6		11.8		0.11	0.1	0.12	0.11
H	2.08	2.08	7.25		10.06		0.1	0.04	0.12	0.06

With equal power and tilt angle, welding speed of 30 mm/s produces a larger molten area than one evaluated with a speed of 40 mm/s; these results are connected with lower heat inputs of the latter welding conditions. With the

same heat input a greater melted area is obtained with 45° tilt angle, guaranteeing better energy absorption; nevertheless, a higher depth of penetration is observed with 30° tilt angle.

Quality checks have been carried out for all of the cross sections; class A quality has been met for the imperfections with reference to international standards for fusion welding of aerospace applications [20], where requirements are given in terms of maximum allowed value for each imperfection, namely 210 μm for undercut.

Microhardness tests have been carried out to verify the extent of the heat affected zone on the extreme conditions of heat input (conditions B and G). An indenting load of 0.300 kgf has been used for a dwell period of 10 s; a 220 μm step has been adopted between two consecutive indentations. The scan paths have been performed at 1 mm from the top surface of the skin and centered respect to the axis of symmetry of the stringer. The results are shown in Figures 11 and 12.

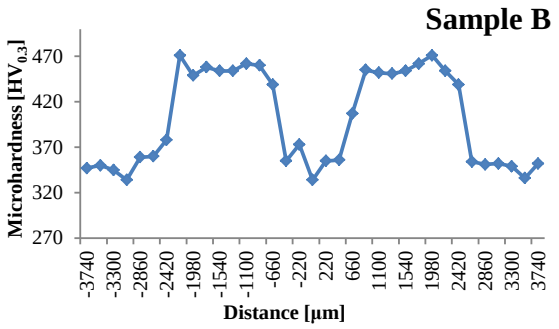

Fig. 11. Microhardness values for T-joint in condition B.

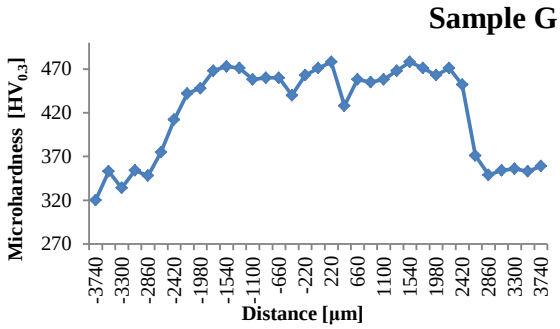

Fig. 12. Microhardness values for T-joint in condition G.

The tests of microhardness show a growing trend of hardness passing from the base material to the molten zone. In the condition B, in which melted areas do not intersect, the microhardness at the axis of symmetry of the stringer presents a decrease with values similar to the base material. Whereas condition G is characterized by a unique melted area, as a consequence uniform higher values compared to base material ones are observed.

Maximum hardness has been found in the fusion zone which, in fact, mainly consists of acicular α' martensite as a consequence of diffusionless transformation of the original β phase, while a mixture of α' and primary α phases is found in the heat affected zone. The increase in hardness as obtained with laser welding is deemed to be reason of improved strength of the welding bead, although proper tensile tests are needed for the assessment. Welding parameters don't directly affect microhardness values, but only the extent of the melted zone and as a consequence the area in which maximum hardness has been observed.

5. Conclusions

Laser welding of 3.2 mm thick plates of Ti-6Al-4V titanium alloy in T-joint configuration has been investigated. The process has been performed in continuous wave emission using a thin disk-laser source. A specific jig has been developed for clamping sheets in test configuration.

Given the fact that beads are found to be uniform, smooth, and silvery, and no spatters are observed, protection has been considered adequate. Welding beads have been examined with a coordinate measuring machine to study distortions. Thermal deformation is a growing function of heat input.

Some isolated pores have been noticed in cross sections, but they present limited size. Analyzed factors have been found to play a noteworthy influence on the responses. Indeed, with equal power and tilt angle, lower welding speed produces a larger molten zone; these results are connected with greater heat inputs. With the same heat input a higher melted area is obtained with 45° tilt angle, guaranteeing better energy absorption.

Class A quality requirements have been met for undercuts. Compared with the base metal, an increase in hardness in the fusion and heat affected zone has been noticed as a consequence of the formation of α' martensite. Future works will deal with testing beads via tensile tests to evaluate mechanical performances.

References

[1] M. J. Donachie, Titanium, A Technical Guide, ASM International, Materials Park, OH, 2000.
[2] X. Cao, M. Jahazi, Effect of Welding Speed on Butt Joint Quality of Ti-6Al-4V Alloy Welded Using a High-Power Nd:YAG Laser, Opt. Laser Eng. 47(11) (2009) 1231–1241.
[3] F. Cardaropoli, V. Alfieri, F. Caiazzo, V. Sergi, Manufacturing of Porous Biomaterials for Dental Implant Applications Through Selective Laser Melting, Adv. Mater. Res. 535–537 (2012) 1222–1229.
[4] L.W. Tsay, C.Y. Tsay, The Effect of Microstructures on the Fatigue Crack Growth in Ti-6Al-4V Laser Welds, Int. J. Fatigue 19(10) (1997) 713–720.
[5] S. Marimuthu, R.M. Eghlio, A.J. Pinkerton, L. Li, Coupled Computational Fluid Dynamic and Finite Element Multiphase Modeling of Laser Weld Bead Geometry Formation and Joint Strengths, ASME J. Manuf. Sci. Eng., 135(1) (2013).
[6] Z. Sun, D. Pan, W. Zhang, Correlation between welding parameters and microstructures in TIG, plasma and laser welded Ti-6Al-4V, in Proceedings of the 6th International Conference Trends inWelding Research, Pine Mountain, Ga, USA, April 2002, pp. 760–767.
[7] H. Liu, K. Nakata, N. Yamamoto, J. Liao, Microstructural characteristics and mechanical properties in laser beam welds of Ti6Al4V alloy, Journal of Materials Science 47(3) (2012) 1460–1470.
[8] S. Wang, X. Wu, Investigation on the microstructure and mechanical properties of Ti-6Al-4V alloy joints with electron beamwelding, Materials and Design 36 (2012) 663–670.
[9] M. Wang, M. Jiang, Q. Wie, K. Gu, Techniques of laser-TIG hybrid T-shape joint welding of titanium alloy, Adv. Mater. Res. 291-294 (2011) 841–847.
[10] R. Spina, D. Sorgente, G. Palumbo, L.D. Scintilla, M. Brandizzi, A.A. Satriano, L. Tricarico, T-joints of Ti alloys with hybrid laser-MIG welding: macro-graphic and micro-hardness analyses, in Proceedings of SPIE "Advances in slow and fast light V", San Francisco, USA, Vol.8239, Article Number 82239C, 2012.
[11] N. Kashaev, V.Ventzke, V. Fomichev, F. Fomin, S. Riekehr, Effect of Nd:YAG laser beam welding on weld morphology and mechanical properties of Ti–6Al–4V butt joints and T-joints, Optics and Lasers in Engineering 86(2016) 172–180.
[12] X. Ma, S. Gong, J. Zhang, W. Lu, J. Yang, Formation, microstructure and mechanical properties of double-sided laser beam welded Ti−6Al−4V T-joint, Trans. Nonferrous Met. Soc. China 26 (2016) 729−735.
[13] A. Giesen, J. Speiser, Fifteen Years of Work on Thin-Disk Lasers: Results and Scaling Laws, J. Sel. Top. Quantum Electron. 13(3) (2007) 598–609.
[14] E. Mastrocinque, G. Corrado, F. Caiazzo, N. Pasquino, V. Sergi, F. Acerra, Disk Laser Welding of Ti6Al4V Alloy, in 21st International Conference on Production Research, Stuttgart, 2011.
[15] F. Caiazzo, E. Mastrocinque, G. Corrado, V. Sergi, Regression Modeling to Predict the Geometrical Features of Ti6Al4V Thin Sheets Butt Joints Welded by Disk Laser, in Proceedings of SPIE Photonics Europe 2012, Bruxelles, Vol. 8433, Paper No. 84330Y1-11, 2012.
[16] W.M. Steen, Laser Material Processing, Springer, London, 157–199, 2003.
[17] W.W. Duley, Laser Welding, John Wiley and Sons, Inc., New York, 1998.
[18] E. Mastrocinque, G. Corrado, F. Caiazzo, N. Pasquino, V. Sergi, Effect of Defocusing on Bead-on-Plate of Ti6Al4V by Yb:YAG Disk Laser, Adv. Mater. Res. 383–390 (2012) 6258–6264.
[19] E. Akman, A. Demir, T. Canel, T. Sinmazcelik, Laser Welding of Ti6Al4V Titanium Alloys, J. Mater. Process. Technol. 209(8) (2009) 3705–3713.
[20] AWS, Specification for Fusion Welding for Aerospace Applications, American Welding Society, Miami, FL, 2001.